Supporting Information

Warren et al. 10.1073/pnas.0910347107

SI Text.

***k* Versus β_2^{H} Plots for $^t\mathrm{Bu_3PhOH}$ and TEMPOH Pseudo-Self-Exchange Reactions.** Plots of $\log(k_{\mathrm{XH/X^\bullet}})$ versus β_2^{H} for (*a*) $^t\mathrm{Bu_3PhO}(^\bullet/\mathrm{H})$ and (*b*) $\mathrm{TEMPO}(^\bullet/\mathrm{H})$ are shown in Fig. S1 (1).

Pseudo-self-exchange reaction of $^t\mathrm{Bu_3PhO^\bullet} + 2,6$-di-tert-butyl-4-methylphenol As mentioned in the main text, the self-exchange rate constant for $^t\mathrm{Bu_3PhOH}$ was determined by studying the pseudo-self-exchange reaction of $^t\mathrm{Bu_3PhO^\bullet} + 2,6$-di-tert-butyl-4-methylphenol (BHT) (Eq. **S1**). This reaction proceeds by initial HAT from BHT to $^t\mathrm{Bu_3PhO^\bullet}$ (Eq. **S1**), with subsequent reaction of the $\mathrm{Me}^t\mathrm{Bu_2PhO}$ radicals with another phenoxyl radical (or $^t\mathrm{Bu_3PhO^\bullet}$) and elimination (Eq. **S2**) (2, 3). ^{1}H NMR spectra of reaction mixtures in all solvents show the formation of $^t\mathrm{Bu_3PhOH}$ and the quinone methide in a 2:1 ratio [the stoichiometry of the net reaction of $\mathrm{Me}^t\mathrm{Bu_2PhO^\bullet}$ (Eq. **S1** + Eq. **S2**)].

The kinetics of reaction **S1** have been measured under pseudo-first-order conditions of excess BHT (5–70 equiv) by using UV-visible (UV-vis) stopped-flow spectrophotometry, following the decay of $^t\mathrm{Bu_3PhO^\bullet}$ ($\lambda_{\max} = 630$ nm). By using $d[^t\mathrm{Bu_3PhO^\bullet}]/dt = 2k_{\mathrm{S1}}[^t\mathrm{Bu_3PhO^\bullet}][\mathrm{BHT}]$ to account for the stoichiometry, $k_{\mathrm{S1}}/\mathrm{M^{-1}\,s^{-1}} = 158 \pm 10\ (\mathrm{CCl_4}),\ 113 \pm 8\ (\mathrm{C_6H_6}),\ 24 \pm 2\ (\mathrm{MeCN})$, and 10 ± 1 (DMSO). The same values are obtained from fitting the spectral data to a more complete kinetic model by using the known dimerization and elimination rate constants (2, 3). The self-exchange rate constants are then derived from the k_{S1} values by using Eq. **S1** (see main text) and $K_{\mathrm{S1}} = 1.45 \pm 0.13$ (data summarized in Table 2, main text). The same method is used to correct k_{S1} in hexane, originally reported by Prokof'ev et al. (4). Our value of $k_{\mathrm{XH/X^\bullet}}(^t\mathrm{Bu_3PhOH})$ in $\mathrm{CCl_4}$ ($130 \pm 20\ \mathrm{M^{-1}\,s^{-1}}$) is smaller than the previously reported value, $220 \pm 20\ \mathrm{M^{-1}\,s^{-1}}$, measured by EPR for $^t\mathrm{Bu_3PhO^\bullet} + 2,4,6\text{-}^t\mathrm{Bu_3}\text{-}3,5\text{-}d_2\text{-PhOH}$ (5). The EPR value is not used here.

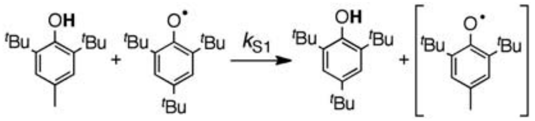

[S1]

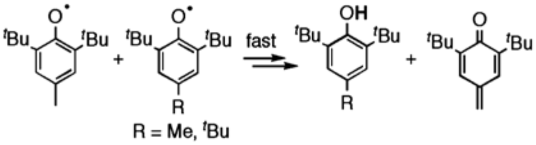

[S2]

$^t\mathrm{Bu_3PhO^\bullet} + \alpha$-tocopherol (TocOH) Kinetics. The rate constant k_{S3} was determined by using stopped-flow spectrophotometry under pseudo-first-order conditions of excess TocOH. The kinetic experiments were carried out as described in the main text. The disappearance of the UV bands of $^t\mathrm{Bu_3PhO^\bullet}$ are accompanied by the growth of the optical spectrum of the α-tocopheroxyl radical ($\mathrm{TocO^\bullet}$) (Fig. S2*a*) (6). The spectra were fit to a first-order kinetic model by using SPECFIT software (7). A plot of the derived first-order rate constants plotted as a function of [TocOH] is linear with a zero intercept (Fig. S2*b*), yielding $k_{\mathrm{S3}} = 8,100 \pm 600\ \mathrm{M^{-1}\,s^{-1}}$.

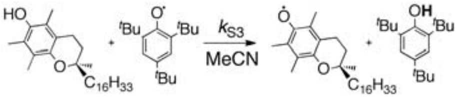

[S3]

$^t\mathrm{Bu_3PhO^\bullet} + 9,10$-Dihydroanthracene (DHA) Kinetics. The disappearance of the optical bands (blue) of $^t\mathrm{Bu_3PhO^\bullet}$ are accompanied by the growth of the optical spectrum of anthracene (Fig. S3). The rate constant k_{S4} was determined by using UV-visible (UV-vis) spectrophotometry under pseudo-first-order conditions of excess DHA by using the following procedure. In an inert atmosphere glovebox, 2-mL aliquots of a 5×10^{-5} M stock solution of $^t\mathrm{Bu_3PhO^\bullet}$ in MeCN were placed in five quartz cuvettes with Kontes Teflon stoppers. Above each Teflon stopper 9,10-Dihydroanthracene (10–500 eq) and 1 mL MeCN were placed, and the apparatus was capped with a rubber septum. Initial UV-vis spectra were taken for each cuvette, and then reactions were initiated by opening the Teflon stopper and mixing the two solutions. The spectra were fit to a first-order kinetic model by using SPECFIT software. A plot of the derived first-order rate constants plotted as a function of [DHA] is linear, with a zero intercept yielding $k = (8.8 \pm 0.8) \times 10^{-3}\ \mathrm{M^{-1}\,s^{-1}}$. With k_{S4} defined as $d[^t\mathrm{Bu_3PhO^\bullet}]/dt = 2k_{\mathrm{S4}}[^t\mathrm{Bu_3PhO^\bullet}][\mathrm{DHA}]$, $k_{\mathrm{S4}} = 4.4 \pm 0.4 \times 10^{-3}\ \mathrm{M^{-1}\,s^{-1}}$. Because there are four equivalent hydrogens in DHA, the rate constant for hydrogen atom transfer per hydrogen is lower than this value by the statistical factor of 4: $k_{\mathrm{XH/Y^\bullet}}(\mathrm{S4}) = 1.1 \pm 0.1 \times 10^{-3}\ \mathrm{M^{-1}\,s^{-1}}$.

[S4]

General Considerations for Determination of Bond Dissociation Free Energies (BDFEs) and $k_{\mathrm{XH/X^\bullet}}$. *Determination of BDFEs.* The homolytic bond strengths discussed below were derived from either gas phase bond dissociation enthalpies (BDEs) or redox potential ($E_{1/2}$) and $\mathrm{p}K_{\mathrm{a}}$ data. BDFEs were derived from gas phase BDEs by using Eqs. **4** and **5** of the main text, as discussed there. Unless otherwise noted, α_2^{H} values were taken from ref. 8, and β_2^{H} values were taken from ref. 9. Free energies of solvation of $\mathrm{H_2}$ in water and organic solvents are from ref. 10 and 11, respectively. Abraham's model also allows conversion of BDFEs between two solvents, by using a modification of Eq. **6** (see main text), as shown by Eq. **S5**. BDFEs derived from $E_{1/2}$ and $\mathrm{p}K_{\mathrm{a}}$ data used Eq. **S6** (12, 13). The constants $C_G = 54.9\ \mathrm{kcal\,mol^{-1}}$ (MeCN, $\mathrm{Cp_2Fe^{+/0}}$ electrochemical reference) and $C_G = 57.6\ \mathrm{kcal\,mol^{-1}}$ (water, NHE electrochemical reference) are discussed in detail in refs. 12 and 13.

$$\mathrm{BDFE_{solv1}} - \mathrm{BDFE_{solv2}} = \Delta\Delta G^\circ_{\mathrm{solv}}(\mathrm{H^\bullet}) + \Delta\Delta G^\circ_{\mathrm{solv}}(\mathrm{X^\bullet}) - \Delta\Delta G^\circ_{\mathrm{solv}}(\mathrm{XH}) \qquad \textbf{[S5]}$$

$$\mathrm{BDFE} = 1.37\mathrm{p}K_{\mathrm{a}} - 23.1E_{1/2} + C_G \qquad \textbf{[S6]}$$

Determination of self-exchange rate constants ($k_{\mathrm{XH/X^\bullet}}$). All self-exchange rate constants or pseudo-self-exchange rate constants were taken from the literature as noted below. Pseudo-self-exchange rate constants were corrected for driving force, where necessary, by using Eq. **8** in the main text. When necessary, self-exchange rate constants were corrected for solvent effects by using Ingold's kinetic solvent effect (KSE) model (Eq. **7**, main text). The relevant α_2^{H} and β_2^{H} values were taken from the sources mentioned above, unless otherwise noted. The KSE model can also be rearranged to convert self-exchange rate constants between two solvents, as shown in

$$\log(k_{\text{solv1}}) - \log(k_{\text{solv2}}) = -8.3\alpha_2^{\text{H}}(\text{XH})[\beta_2^{\text{H}}(\text{solv1}) - \beta_2^{\text{H}}(\text{solv2})] \qquad [\mathbf{S7}]$$

Bond Strengths for Bulky Phenols. Gas phase BDEs for all phenols used in this study can be found in ref. 14. These were converted to solution BDFEs in the appropriate solvent by using the two-step method described in the main text. β_2^{H} for bulky phenols is approximated as ~0.15. Following Ingold (15), the phenoxyl radical is expected to be somewhat H-bond accepting because of the quinoid-like resonance form. However, because of the steric bulk of the 2,6-di-*tert*-butyl substitution we cannot simply approximate β_2^{H} as a ketone (~0.48). Instead, we linearly extrapolate β_2^{H} for bulky phenols from benzoquinone ($\beta_2^{\text{H}} = 0.48$), because 2,4,6-tri-*tert*-butyl phenol has $\alpha_2^{\text{H}} = 0.22$, about one-third of $\alpha_2^{\text{H}}(\text{PhOH}) = 0.6$. This is reasonable because a similar (factor of 3) decrease in β_2^{H} is observed going from pyridine to 2,6-di-*tert*-butyl pyridine (9). For 2,6-dimethyl substitution (e.g., tocopherols) there is no dramatic shift in β_2^{H} from the unsubstituted derivative.

The bond strengths differ slightly from previous reports from our group (12). For example, from a variety of literature data Mader et al. derived $\text{BDFE}_{\text{MeCN}}({}^t\text{Bu}_3\text{PhOH}) = 77 \pm 1$ kcal mol^{-1}. Starting from $\text{BDE}_g({}^t\text{Bu}_3\text{PhOH}) = 79.9$ kcal mol^{-1} we derive $\text{BDFE}_{\text{MeCN}}({}^t\text{Bu}_3\text{PhOH}) = 77.8 \pm 1.0$ kcal mol^{-1}, slightly larger but within error of our previously reported value. For other solvents (e.g., C_6H_6, DMSO, and CCl_4) the Abraham model predicts BDFEs within ≤ 0.5 kcal mol^{-1} of those derived by other methods, like thermochemical cycles. Because the Abraham model is so accurate for most phenols, and for consistency in this study, the BDFEs for bulky phenols are all derived from the respective gas phase values by using the Abraham model.

Trolox C Bond Strength and Self-Exchange Rate Constant. Trolox C, (±)-6-Hydroxy-2,5,7,8-tetramethylchromae-2-carboxylic-acid, is a water soluble tocopherol analogue. The $\text{p}K_{\text{a}}$ of Trolox C is 12.1, and the one electron reduction potential of the phenoxide is 0.192 V versus NHE (16, 17). Using these data in Eq. **S6** gives $\text{BDFE}(\text{Trolox}) = 78.5 \pm 1.0$ kcal mol^{-1} in water.

The self-exchange rate constant for Trolox C in water can calculated from the self-exchange rate constant for α-tocopherol in MeCN (see below), assuming the properties of Trolox and tocopherol are about the same. This is a reasonable assumption based on their very similar structures. By using $\alpha_2^{\text{H}}(\text{TocOH}) = 0.37$ (18), $\beta_2^{\text{H}}(\text{MeCN}) = 0.44 \pm 0.03$, and $\beta_2^{\text{H}}(\text{H}_2\text{O}) = 0.38 \pm 0.04$, $\log k_{\text{XH/X}^\bullet}(\text{Trolox C}) = 4.53 \pm 0.55$ or $k_{\text{XH/X}^\bullet} \sim 3.4 \times 10^4$ M^{-1} s^{-1}.

Phenol Bond Strength and Self-Exchange Rate Constant. The gas phase BDE of phenol has recently been critically reviewed to be 88.7 ± 0.5 kcal mol^{-1} (19), corresponding to $\text{BDFE}(\text{PhOH})_{(g)} = 80.6 \pm 0.5$ kcal mol^{-1} at 298 K. For the BDFE in di-*tert*-butyl peroxide (DTBP) solution $\Delta G^\circ_{\text{solv}}(\text{PhOH}) - \Delta G^\circ_{\text{solv}}(\text{PhO}^\bullet)$ is calculated by using $\alpha_2^{\text{H}}(\text{PhOH}) = 0.596 \pm 0.015$, $\beta_2^{\text{H}}(\text{DTBP}) = 0.35 \pm 0.1$ (20), and $\alpha_2^{\text{H}}(\text{DTBP}) = 0$. Ingold and coworkers have previously approximated $\beta_2^{\text{H}}(\text{PhO}^\bullet) \sim \beta_2^{\text{H}}(\text{RC(O)R}) = 0.48 \pm 0.04$, which is reasonable upon the basis of the primary quinoid-like resonance structure of the phenoxyl radical (15). We approximate $\Delta G^\circ_{\text{solv}}(\text{H}^\bullet) \sim \Delta G^\circ_{\text{solv}}(\text{H}_2)$, following Roduner (21). We will also assume that $\Delta G^\circ_{\text{solv}}(\text{H}_2)$ in DTBP is approximately that of MeCN (5.12 kcal mol^{-1}), because the free energy of solvation of H_2 does not vary widely in polar, aprotic media (11). Substitution of these values into Eq. **S6** gives $\text{BDFE}_{\text{DTBP}}(\text{PhOH}) = 87.8 \pm 1.1$ kcal mol^{-1}. The same type of analysis in water ($\alpha_2^{\text{H}} = 0.35 \pm 0.02$, $\beta_2^{\text{H}} = 0.38 \pm 0.02$) gives $\text{BDFE}_{\text{water}}(\text{PhOH}) = 90.1 \pm 1.0$ kcal mol^{-1}.

Alternatively, $\text{BDFE}_{\text{water}}(\text{PhOH})$ can be derived from aqueous thermochemical data. Lind and coworkers reported the reduction potential for the phenoxyl radical in water as 0.79 ± 0.01 V versus NHE and $\text{p}K_{\text{a}}(\text{PhOH}) = 10.0$ (22). Application of Eq. **S6** gives $\text{BDFE}_{\text{water}}(\text{PhOH}) = 89.4 \pm 1.0$ kcal mol^{-1}, in quantitative agreement with the above derivation from gas phase data.

The self-exchange rate constant for phenol is estimated from the pseudo-self-exchange reaction of phenoxyl with 2-naphthol. Foti and coworkers have determined that the rate constant for this reaction in 3:1 (vol/vol) in DTBP:benzene is $(4.5 \pm 0.6) \times 10^6$ M^{-1} s^{-1} (23). Given the difference in the β_2^{H} value of DTBP ($\beta_2^{\text{H}} = 0.35$) and benzene ($\beta_2^{\text{H}} = 0.14$), the phenols predominantly hydrogen bond with DTBP. Thus, we will make the simplifying approximation that this reaction was measured in a solvent with $\beta_2^{\text{H}} \sim 0.35$. By using the BDFEs for PhOH and 2-naphthol (see below), $\Delta G^\circ = -1.9 \pm 1.5$ kcal mol^{-1} corresponding to $\log K = 1.4 \pm 1.1$. Using Eq. **8**, as outlined in the main text, gives $k_{\text{XH/X}^\bullet}(\text{PhOH}) = 9.4 \times 10^5$ M^{-1} s^{-1}. Because of the uncertainty in the bond strengths, and therefore K_{eq}, the error bars on this value are *ca.* one order of magnitude. For the purposes of our analysis we use the value $k_{\text{XH/X}^\bullet}(\text{PhOH}) = 9 \times 10^5$ M^{-1} s^{-1}, which assumes that the HAT self-exchange rate constants for phenol and 2-naphthol are similar, which is reasonable within the factor-of-ten error bars (the naphthol may have a slightly smaller inner-sphere reorganization energy because of the larger aromatic ring).

1-Naphthol and 2-Naphthol Bond Strengths and Self-Exchange Rate Constants. The gas phase BDE for 1-naphthol (1-NapOH) is 83.5 kcal mol^{-1}, from Borges dos Santos et al.'s compilation of gas phase BDEs derived from reported experimental and computational values (14). Conversion to gas phase BDFE gives $\text{BDFE}_g(\text{1-NapOH}) = 75.4$ kcal mol^{-1}. For the BDFE in DTBP solution, the same method as for PhOH is followed, with $\alpha_2^{\text{H}}(\text{1-NapOH}) = 0.608 \pm 0.013$ and $\beta_2^{\text{H}}(\text{1-NapO}^\bullet) \sim \beta_2^{\text{H}}(\text{RC(O)R}) = 0.48 \pm 0.04$. This yields $\text{BDFE}_{\text{DTBP}}(\text{1-NapOH}) = 82.6 \pm 1.1$ kcal mol^{-1}. A similar analysis in water ($\alpha_2^{\text{H}} = 0.38 \pm 0.02$, $\beta_2^{\text{H}} = 0.35 \pm 0.02$) gives $\text{BDFE}_{\text{water}}(\text{1-NapOH}) = 85.0 \pm 1.2$ kcal mol^{-1}.

Similarly, the gas phase $\text{BDE}(\text{2-NapOH}) = 86.8$ kcal mol^{-1} corresponding to $\text{BDFE}_g(\text{2-NapOH}) = 78.7$ kcal mol^{-1}. For the BDFE in DTBP solution the same method as for PhOH is followed, with $\alpha_2^{\text{H}}(\text{2-NapOH}) = 0.612 \pm 0.013$ and $\beta_2^{\text{H}}(\text{2-NapO}^\bullet) \sim \beta_2^{\text{H}}(\text{RC(O)R}) = 0.48 \pm 0.04$. This yields $\text{BDFE}_{\text{DTBP}}(\text{2-NapOH}) = 85.9 \pm 1.1$ kcal mol^{-1}. A similar analysis in water gives $\text{BDFE}_{\text{water}}(\text{2-NapOH}) = 88.3 \pm 1.2$ kcal mol^{-1}.

Das and Neta have reported the aqueous $\text{p}K_{\text{a}}$ and $E_{1/2}$ values necessary for derivation of aqueous BDFEs (24). From these data, $\text{BDFE}_{\text{water}}(\text{1-NapOH}) = 83.9 \pm 1.0$ kcal mol^{-1} and $\text{BDFE}_{\text{water}}(\text{2-NapOH}) = 86.7 \pm 1.0$ kcal mol^{-1}. These values are not used in the main text but serve to benchmark our use of the Abraham model to determine solution BDFEs from gas phase BDE data. For PhOH, 1-NapOH, and 2-NapOH the two independent BDFE derivations are within error of each other, which indicates that the Abraham model (and associated approximations) is a reasonable method by which to estimate solution BDFEs.

The self-exchange rate constants for 1-NapOH and 2-NapOH are approximated to be the same as that for PhOH within the factor-of-ten error bars, as noted above. For 1-NapOH, the likely smaller reorganization energy is probably balanced by the greater steric hindrance to HAT. Thus, for further analysis we approximate $k_{\text{XH/X}^\bullet}(\text{PhOH}) = k_{\text{XH/X}^\bullet}(\text{2-NapOH}) \sim k_{\text{XH/X}^\bullet}(\text{1-NapOH}) \sim k_{\text{XH/X}^\bullet}(\text{PhOH}) \sim 9 \times 10^5$ M^{-1} s^{-1}.

Tyrosine Bond Strength and Self-Exchange Rate Constant. The one electron reduction potential of the tyrosyl radical was determined by Lind and coworkers, as $E° = 0.71 \pm 0.02$ V versus NHE (25). The pK_a of the phenolic proton in tyrosine is 10.1 (26). Application of Eq. **S6** gives BDFE(tyrosine) $= 87.8 \pm 1.0$ kcal mol^{-1}.

The H-atom self-exchange rate constant for tyrosine is not expected to be significantly different than that of phenol, because of the structural similarities of the compounds. For example, the rate constant for H-abstraction from Trolox C is about the same for both phenoxyl and tyrosyl radicals (27). Thus, for further discussion, $k_{\mathrm{XH/X}^\bullet}$(tyrosine)$\approx k_{\mathrm{XH/X}^\bullet}$(phenol). The $\beta_2{}^{\mathrm{H}}$ values of water ($\beta_2{}^{\mathrm{H}} = 0.38 \pm 0.02$) and DTBP ($\beta_2{}^{\mathrm{H}} = 0.35 \pm 0.1$) are the same within error, so no correction for H bonding is necessary yielding $k_{\mathrm{XH/X}^\bullet}$(tyrosine) $= 9 \times 10^5$ M^{-1} s^{-1}.

***tert*-Butyl Hydroperoxide Bond Strength and Self-Exchange Rate Constant.** Previous work from our group (28) has used BDE$_g$(^{t}BuOOH) $= 89$ kcal mol^{-1}, as reported by Benson (29). More recent data indicate that this value is too high. Simmie et al. recently gave ΔH_f°(^{t}BuOO$^\bullet$) $= -24.69$ kcal mol^{-1} (30), which, together with ΔH_f°(H$^\bullet$) $= 52.103$ kcal mol^{-1} (31) and ΔH_f°(^{t}BuOOH) $= -56.14$ kcal mol^{-1} (32), gives BDE$_g$(^{t}BuOOH) $=$ 83.6 kcal mol^{-1}. Another recent measurement of ΔH_f°(^{t}BuOO$^\bullet$) gives a similar result (33). A BDE$_g$(^{t}BuOOH) $= 85 \pm 2$ kcal mol^{-1} was derived by Clifford et al. by using gas phase measurements of the ionization energy and gas phase acidity (34). Finally, recent density functional theory calculations using CBS-QB3 or CBS-APNO basis sets gave BDE$_g$(^{t}BuOOH) $=$ 84.85 kcal mol^{-1} and BDE$_g$(^{t}BuOOH) $= 83.89$ kcal mol^{-1}, respectively (30). These values are all in reasonable agreement and give a consensus BDE$_g$(^{t}BuOOH) $= 84.3 \pm 1.0$ kcal mol^{-1} (almost 5 kcal mol^{-1} less than that given by Benson), which corresponds to BDFE$_g$(^{t}BuOOH) $= 76.1$ kcal mol^{-1}.

In a non-hydrogen bonding solvent (e.g., isopentane) $\beta_2{}^{\mathrm{H}}$(solvent) $= \alpha_2{}^{\mathrm{H}}$(solvent) $= 0$. Using $\Delta G_{\mathrm{solv}}(\mathrm{H}_2)_{\mathrm{hexane}} =$ 4.30 kcal mol^{-1} gives BDFE$_{\mathrm{alkane}}$(^{t}BuOOH) $= 80.4 \pm 1.0$ kcal mol^{-1}. To determine BDFEs in polar solvents $\alpha_2{}^{\mathrm{H}}$(^{t}BuOOH) and $\beta_2{}^{\mathrm{H}}$(^{t}BuOO$^\bullet$) are needed. Ingold et al. have reported $\alpha_2{}^{\mathrm{H}}$(^{t}BuOOH) $= 0.442$ (errors not given; we estimate ± 0.04) (18). ^{t}BuOO$^\bullet$ is a reasonably good H-bond acceptor ($\beta_2{}^{\mathrm{H}} = 0.19$), as measured by Mugnaini et al. (35). These data, using Abraham's model, allow determination of BDFEs in ethanol ($\alpha_2{}^{\mathrm{H}} = 0.33$, $\beta_2{}^{\mathrm{H}} = 0.44$), BDFE$_{\mathrm{ethanol}}$(^{t}BuOOH) $= 82.6 \pm 1.1$ and styrene ($\alpha_2{}^{\mathrm{H}} = 0$, $\beta_2{}^{\mathrm{H}} = 0.18$), BDFE$_{\mathrm{styrene}}$(^{t}BuOOH) $= 81.7 \pm 1.1$ kcal mol^{-1}.

The self-exchange reaction of ^{t}BuOOH/^{t}BuOO$^\bullet$ has not been directly measured, to our knowledge. Chenier and Howard have measured the HAT reaction of ^{t}BuOO$^\bullet$ and *sec*-butyl hydroperoxide in isopentane, $k = 485$ M^{-1} s^{-1} at 294 K (36). This pseudo-self-exchange reaction is expected to be roughly isoergic (30) and can be taken as $k_{\mathrm{XH/X}^\bullet}$ without correction for driving force. Errors are taken to be *ca.* 20%, giving $k_{\mathrm{XH/X}^\bullet}$(^{t}BuOOH) $= 500 \pm$ 100 M^{-1} s^{-1} in alkane solvents. Using Ingold's KSE model (Eq. **7**) gives $k_{\mathrm{XH/X}^\bullet}$(^{t}BuOOH) $= 12$ M^{-1} s^{-1} in ethanol and $k_{\mathrm{XH/X}^\bullet}$(^{t}BuOOH) $= 110$ M^{-1} s^{-1} in styrene.

***tert*-Butanol Bond Strength and Self-Exchange Rate Constant.** The gas phase BDE of *t*-butanol has recently been reported as 106.3 kcal mol^{-1} (37) corresponding to BDFE$_g$(^{t}BuOH) $=$ 98.1 kcal mol^{-1}. *tert*-butanol has $\alpha_2{}^{\mathrm{H}} = 0.32 \pm 0.04$ (8). Again approximating $\Delta G_{\mathrm{solv}}(\mathrm{H}_2)_{\mathrm{DTBP}}$ as $\Delta G_{\mathrm{solv}}(\mathrm{H}_2)_{\mathrm{MeCN}} = 5.12$ kcal mol^{-1} gives BDFE$_{\mathrm{DTBP}}$(^{t}BuOH) $= 104.4 \pm 1.5$ kcal mol^{-1}.

The hydrogen transfer pseudo-self-exchange rate constant for ^{t}BuO$^\bullet$ + ^{t}Bu$_3$COH in DTBP has been reported by Griller and Ingold as $k_{\mathrm{XH/X'}^\bullet} = 3 \times 10^4$ M^{-1} s^{-1} (38). We will approximate this as the true self-exchange rate constants because ^{t}BuOH and ^{t}Bu$_3$COH are structurally similar.

***L*-Ascorbate Bond Strength, Self-Exchange Rate Constant, and $\alpha_2{}^{\mathrm{H}}$.** The BDFE of AscH$^-$ in acetonitrile solvent has been reported from equilibrium studies with TEMPO (BDFE $= 66.5$ kcal mol^{-1}), BDFE(AscH$^-$) $= 67.8 \pm 1.0$ kcal mol^{-1} (39). By using available aqueous thermochemical data BDFE$_{\mathrm{water}}$ (AscH$^-$) $= 73.6 \pm 1.1$ kcal mol^{-1} (40).

To our knowledge no direct measurement of the ascorbate/ascorbyl radical H-atom self-exchange rate constant has been reported. As with the tocopherol/tocopheroxyl radical HAT self-exchange rate constant (see above), we turn to the Marcus cross relation in order to estimate $k_{\mathrm{XH/X}^\bullet}$(AscH$^-$), by using the roughly isoergic cross reaction between TEMPO and 5,6-isopropylidene ascorbate (*i*AscH$^-$). The rate and equilibrium constants for this reaction (Eq. **S8**) are $1{,}720 \pm 150$ M^{-1} s^{-1} and 1.2 ± 0.2, respectively (39). The self-exchange rate constant for TEMPOH has $k_{\mathrm{XH/X}^\bullet} = 4.7 \pm 1.0$ M^{-1} s^{-1} (41). Application of Eq. **2** and taking $f = 1$ gives $k_{\mathrm{XH/X}^\bullet}(\mathrm{AscH}^-)_{\mathrm{MeCN}} = (5.4 \pm 1.2) \times 10^5$ M^{-1} s^{-1}. Using the $\alpha_2{}^{\mathrm{H}}$(AscH$^-$) $= 0.3$ (see below) gives $k_{\mathrm{XH/X}^\bullet}$(AscH$^-$)$_{\mathrm{water}} = 3 \times 10^4$ M^{-1} s^{-1}.

An $\alpha_2{}^{\mathrm{H}}$ value for AscH$^-$ has not been reported to our knowledge. By using kinetic data for *i*AscH$^-$ + TEMPO and AscH$^-$ + TEMPO (42) in MeCN and DMSO, we can make a crude estimate of $\alpha_2{}^{\mathrm{H}}$(AscH$^-$) (Fig. S5). Using the KSE model requires that the slope of the fit lines equals $-8.3\alpha_2{}^{\mathrm{H}}$(AscH$^-$). The average of the slopes for *i*AscH$^-$ and AscH$^-$ is -2.25, corresponding to $\alpha_2{}^{\mathrm{H}}$(AscH$^-$) $= 0.3$. Whereas this is only an estimate, it is consistent with $\alpha_2{}^{\mathrm{H}}$ values for other secondary alcohols (~0.32) (8).

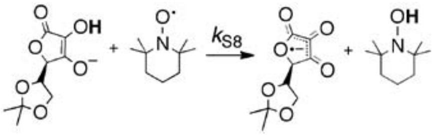

[S8]

Toluene Bond Strength and Self-Exchange Rate Constant. The gas phase BDE of toluene is reported as 89.8 ± 0.6 kcal mol^{-1} (43). Toluene and the benzyl radical are not expected to interact strongly with solvent, and thus their free energies of solvation will be roughly equivalent. The gas phase BDE needs only to be corrected for TS_f°(H$^\bullet$) and $\Delta G_{\mathrm{solv}}^\circ$(H$_2$). For toluene in DTBP this yields BDFE$_{\mathrm{DTBP}} = 86.8 \pm 1.0$ kcal mol^{-1}. The H-atom self-exchange reaction has been briefly described by Jackson and O'Neil as $k_{\mathrm{XH/X}^\bullet}$(PhCH$_3$) $= 8 \times 10^{-5}$ M^{-1} s^{-1} (44). As above, both toluene and the benzyl radical are expected to interact (hydrogen bond) only weakly with solvent, so the self-exchange rate constant should be roughly independent of solvent.

9,10-Dihydroanthracene Bond Strength and Self-Exchange Rate Constant. The BDFE of DHA can be calculated from thermochemical data reported by Bordwell and coworkers in DMSO (45). DHA has p$K_a = 30.1$, and the conjugate base of DHA has $E_{1/2} =$ -1.575 V versus Cp$_2$Fe$^{+/0}$. Application of Eq. **S6** with $C_G = 71.1$ kcal mol^{-1} gives BDFE$_{\mathrm{DMSO}}$(DHA) $= 76.1 \pm 1.0$ kcal mol^{-1}. Because the neutral and radical are not expected to strongly interact with the solvent, the BDFE only needs to be corrected for ΔG_{solv}(H$_2$) to interconvert the BDFE in DMSO to BDFEs in other solvents.

The H-atom self-exchange rate constant for DHA has been be estimated to be $k_{\mathrm{XH/X}^\bullet} = 5 \times 10^{-5}$ M^{-1} s^{-1} in MeCN by using the Marcus cross relation for the oxidation of DHA by 2,2′-biimidazoline complexes of Fe$^{\mathrm{II}}$ (46). As for the case with toluene, this self-exchange rate constant is not expected to vary with solvent.

Derivation of the Solvent Correction (C_S) Term. As noted in the main text, the Marcus theory of electron transfer (ET), from which the CR is derived, applies to unimolecular reactions of weakly bound precursor and successor complexes. In the case of ET reactions, precursor/successor complex formation is often simply estimated as the electrostatic work to bring together the ionic charges. In contrast, HAT reactions involve no net change in charge, so the electrostatic term is not needed. However, HAT reactions have distinct configurations because H transfer occurs over very short distances.

In this light, a more complete analysis of an HAT reaction is given in Scheme S1, for reactants and products that are H-bond donors and a H-bond-accepting solvent (S). It should be noted that Scheme S1 does not describe reactions whose rates approach the diffusion limit, so that the preequilibria in ${K_{\mathrm{X}}}^{S}$ and K_{P} can no longer be considered rapid relative to $k^{0}_{\mathrm{XH/Y}\bullet}$. Starting with the assumption that the CR holds for the unimolecular HAT step, $k^{0}_{\mathrm{XH/Y}\bullet}$, a more complete kinetic expression can be derived using the KSE model to relate the k^{0} values to the measured k^{S} values and with ${K_{\mathrm{XH/Y}\bullet}}^{0} = K^{\mathrm{S}}_{\mathrm{XH}/Y\bullet}(K^{\mathrm{S}}_{\mathrm{YH}}K_{\mathrm{S}}/K^{\mathrm{S}}_{\mathrm{XH}}K_{\mathrm{P}})$. K_{S} and K_{P} are the equilibrium constants for precursor and successor complex formation, respectively, and K_{X} and K_{Y} are the equilibrium constants for 1:1 complex formation of solvent (S) with XH or YH, respectively. The result can be written in the form of the CR with a correction term C_{S} that includes the various equilibrium constants (below).

Scheme S1 is a more complete treatment and more conceptually correct, but it is more complex in its application and typically not needed. The accuracy of the CR with the C_{S} correction, for the 30 reactions in aprotic solvents in Table 4 (main text) for which the Abraham model can be used to estimate the equilibrium constants, is comparable to the simpler treatment above, with an average deviation of 4.0. The C_{S} correction is typically small, usually within the error bars of each individual rate constant (Table S3). For HAT from O—H bonds, the average $\log(C_{\mathrm{S}}) = 0.3 \pm 0.1$, a factor of 2 in k_{calc}. The effect is more significant for abstractions from C—H bonds, $\log(C_{\mathrm{S}}) = 0.9 \pm 0.1$, a factor of 8, due to the large difference in H bonding for R—H ($\alpha_2^{\mathrm{H}} = 0$) and ROH. Reactions in protic media are more complex, as noted above, because hydrogen bonds from solvent to the oxyl radical can be important. For example, based on the $\alpha_2^{\mathrm{H}}(\mathrm{TEMPO}) = 0.46$, the H bonding from water to TEMPO is nearly as large as that from TEMPOH to water. In sum, the CR with C_{S} is a more complete treatment that may be preferred when there is a large variation in α_2^{H} values and in protic solvents, but the simpler CR/KSE model gives excellent agreement in most cases.

We start from the Marcus cross relation without solvent corrections:

$$k_{\mathrm{XH/Y^{\bullet}}}{}^{0} = \sqrt{k_{\mathrm{XH/X^{\bullet}}}{}^{0}\,k_{\mathrm{YH/Y^{\bullet}}}{}^{0}\,K_{\mathrm{XH/Y^{\bullet}}}{}^{0}f}$$

and use an equivalent form of Ingold's KSE model:

$$k_{\mathrm{XH/Y^{\bullet}}}{}^{S} = k_{\mathrm{XH/Y^{\bullet}}}{}^{0}({K_{\mathrm{X}}}^{S})^{-1}$$

where ${K_{\mathrm{X}}}^{S}$ describes the equilibrium of H-bond formation between substrate and solvent (see Scheme S1 below).

Substitution gives

$$k_{\mathrm{XH/Y^{\bullet}}}{}^{S} = \frac{\sqrt{k_{\mathrm{XH/X^{\bullet}}}{}^{0}\,k_{\mathrm{YH/Y^{\bullet}}}{}^{0}\,K_{\mathrm{XH/Y^{\bullet}}}{}^{0}f}}{{K_{\mathrm{X}}}^{S}}$$

The Ingold KSE model for self-exchange reactions gives

$$k_{\mathrm{XH/X^{\bullet}}}{}^{0} = k_{\mathrm{XH/X^{\bullet}}}{}^{S}{K_{\mathrm{X}}}^{S} \ \text{ and } \ k_{\mathrm{YH/Y^{\bullet}}}{}^{0} = k_{\mathrm{YH/Y^{\bullet}}}{}^{S}{K_{\mathrm{Y}}}^{S}$$

where ${K_{\mathrm{X}}}^{S}$ and ${K_{\mathrm{Y}}}^{S}$ describe the equilibrium of H-bond formation between substrate and solvent.

Again, substitution gives

$$k_{\mathrm{XH/Y^{\bullet}}}{}^{S} = \sqrt{k_{\mathrm{XH/X^{\bullet}}}{}^{S}\,k_{\mathrm{YH/Y^{\bullet}}}{}^{S}\,K_{\mathrm{XH/Y^{\bullet}}}{}^{0}f}\sqrt{\frac{{K_{\mathrm{Y}}}^{S}}{{K_{\mathrm{X}}}^{S}}}$$

To convert $K_{\mathrm{XH/Y^{\bullet}}}{}^{0}$ into $K_{\mathrm{XH/Y^{\bullet}}}{}^{S}$, Scheme S1 is used:

$$K_{\mathrm{XH/Y^{\bullet}}}{}^{0} = \frac{{K_{\mathrm{Y}}}^{S}K_{S}}{{K_{\mathrm{X}}}^{S}K_{P}}K_{\mathrm{XH/Y^{\bullet}}}{}^{S}$$

Substitution gives

$$k_{\mathrm{XH/Y^{\bullet}}}{}^{S} = \sqrt{k_{\mathrm{XH/X^{\bullet}}}{}^{S}\,k_{\mathrm{YH/Y^{\bullet}}}{}^{S}\,K_{\mathrm{XH/Y^{\bullet}}}{}^{S}f}\,\frac{{K_{\mathrm{Y}}}^{S}}{{K_{\mathrm{X}}}^{S}}\sqrt{\frac{K_{S}}{K_{P}}}$$

giving

$$k_{\mathrm{XH/Y^{\bullet}}}{}^{S} = \sqrt{k_{\mathrm{XH/X^{\bullet}}}{}^{S}\,k_{\mathrm{YH/Y^{\bullet}}}{}^{S}\,K_{\mathrm{XH/Y^{\bullet}}}{}^{S}f}\,C_{S} \ \text{ with } C_{S} = \frac{{K_{\mathrm{Y}}}^{S}}{{K_{\mathrm{X}}}^{S}}\sqrt{\frac{K_{S}}{K_{P}}}$$

$$\log C_{S} = \log {K_{\mathrm{Y}}}^{S} - \log {K_{\mathrm{X}}}^{S} + \frac{1}{2}\log K_{S} - \frac{1}{2}\log K_{P}$$

From Ingold's model:

$$\log {K_{\mathrm{X}}}^{S} = 8.3{\alpha_2}^{\mathrm{H}}(\mathrm{XH}){\beta_2}^{\mathrm{H}}(\mathrm{S})$$

and

$$\log {K_{\mathrm{Y}}}^{S} = 8.3{\alpha_2}^{\mathrm{H}}(\mathrm{YH}){\beta_2}^{\mathrm{H}}(\mathrm{S})$$

From Abraham's model:

$$\log K_{P} = 7.35[{\alpha_2}^{\mathrm{H}}(\mathrm{XH}){\beta_2}^{\mathrm{H}}(\mathrm{Y}^{\bullet})] - 1.094$$

and

$$\log K_{S} = 7.35[{\alpha_2}^{\mathrm{H}}(\mathrm{YH}){\beta_2}^{\mathrm{H}}(\mathrm{X}^{\bullet})] - 1.094$$

Substitution gives

$$\begin{aligned}\log C_{S} = {} & 8.3{\alpha_2}^{\mathrm{H}}(\mathrm{XH}){\beta_2}^{\mathrm{H}}(\mathrm{S}) - 8.3{\alpha_2}^{\mathrm{H}}(\mathrm{YH}){\beta_2}^{\mathrm{H}}(\mathrm{S}) \\ & + 3.68({\alpha_2}^{\mathrm{H}}(\mathrm{XH}){\beta_2}^{\mathrm{H}}(\mathrm{Y}^{\bullet})) - 0.55 \\ & - 3.68({\alpha_2}^{\mathrm{H}}(\mathrm{YH}){\beta_2}^{\mathrm{H}}(\mathrm{X}^{\bullet})) + 0.55\end{aligned}$$

and

$$\begin{aligned}\log C_{S} = {} & 8.3{\beta_2}^{\mathrm{H}}(\mathrm{S})[{\alpha_2}^{\mathrm{H}}(\mathrm{XH}) - {\alpha_2}^{\mathrm{H}}(\mathrm{YH})] \\ & + 3.68[{\alpha_2}^{\mathrm{H}}(\mathrm{XH}){\beta_2}^{\mathrm{H}}(\mathrm{Y}^{\bullet}) - {\alpha_2}^{\mathrm{H}}(\mathrm{YH}){\beta_2}^{\mathrm{H}}(\mathrm{X}^{\bullet})]\end{aligned}$$

Summary of BDFE and Self-Exchange Rate Constants as a Function of Solvent. A summary of BDFE and self-exchange rate constants as a function of a solvent can be found in Table S1.

Evidence for a Concerted Mechanism for Reaction 11. Thermochemical data in MeCN ($Cp_2Fe^{+/0}$ electrochemical reference) (47). See also Fig. S6, below.

$$\begin{aligned} E_{1/2}({}^t\mathrm{Bu_3PhOH}^{\bullet+/0}) &= 0.94\ \mathrm{V}, & E_{1/2}(\mathrm{TEMPOH}^{\bullet+/0}) &= 0.71\ \mathrm{V}, \\ E_{1/2}({}^t\mathrm{Bu_3PhO}^{\bullet/-}) &= -0.71\ \mathrm{V}, & E_{1/2}(\mathrm{TEMPO}^{\bullet/-}) &= -1.91\ \mathrm{V}, \\ \mathrm{p}K_\mathrm{a}({}^t\mathrm{Bu_3PhOH}) &= 28, & \mathrm{p}K_\mathrm{a}(\mathrm{TEMPOH}) &= 41, \\ \mathrm{p}K_\mathrm{a}({}^t\mathrm{Bu_3PhOH}^{\bullet+})_\mathrm{calc} &= 0.3, & \mathrm{p}K_\mathrm{a}(\mathrm{TEMPOH}^{\bullet+})_\mathrm{calc} &= \sim-3. \end{aligned}$$

Summary of Observed and Calculated (Eq. 2) Hydrogen Transfer Rate Constants. A summary of observed and calculated (Eq. **2**) hydrogen transfer rate constants can be found in Table S2.

Summary of C_S Values and C_S-Corrected Rate Constants. A summary of C_S values and C_S-corrected rate constants can be found in Table S3.

Comparison of k_{obs} and k_{calc} with C_S Corrections. A comparison of k_{obs} and k_{calc} with C_S corrections can be found in Fig. S7.

1. α_2^H determined as discussed in the main text. See also Abraham MH, Abraham RJ, Byrne J, Griffiths L (2006) NMR method for the determination of solute hydrogen bond acidity. *J Org Chem* 71:3389–3394.
2. Lucarini M, Pedulli GF, Cipollone M (1994) Bond dissociation enthalpy of -tocopherol and other phenolic antioxidants. *J Org Chem* 59:5063–5070.
3. Coronel MEJ (2005) Alkyl substituted phenoxyl decay in a hydrogen transfer equilibrium. *Int J Chem Kinet* 37:1–4.
4. Prokof'ev AI, Malysheva NA, Bubnov NN, Solodovnikov SP, Kabachnik MI (1976) Investigation of fast reactions of sterically hindered aroxyl radicals. *B Acad Sci USSR Ch+* 25:494–497.
5. Arick MR, Weissman SI (1968) Direct measurement of the rate of hydrogen-atom exchange between a phenol and its phenoxyl radical. *J Am Chem Soc* 90:1654.
6. Gregor W, Grabner G, Adelwöhrer C, Rosenau T, Gille L (2005) Antioxidant properties of natural and synthetic chromanol derivatives: Study by fast kinetics and electron spin resonance spectroscopy. *J Org Chem* 70:3472–3483.
7. Binstead RA, Zuberbühler AD, Jung B (2006) SPECFIT, version 3.0.38 (Spectrum Software Associates, Chapel Hill).
8. Abraham MH, et al. (1989) Hydrogen bonding. Part 7. A scale of solute hydrogen-bond acidity based on log *K* values for complexation in tetrachloromethane. *J Chem Soc Perk T2* 1989:699–711.
9. Abraham MH, Grellier PL, Prior DV, Morris JJ, Taylor PJ (1990) Hydrogen bonding. Part 10. A scale of solute hydrogen-bond basicity using log *K* values for complexation in tetrachloromethane. *J Chem Soc Perk T2* 1990:521–529.
10. Young CL, ed (1981) *Hydrogen and Deuterium*, IUPAC Solubility Data Series (Permagon, New York), Vols. 5/6.
11. Brunner E (1985) Solubility of hydrogen in 10 organic solvents at 298.15, 323.15, and 373.15 K. *J Chem Eng Data* 30:269–273.
12. Mader EA, et al. (2009) Trends in ground-state entropies for transition metal based hydrogen atom transfer reactions. *J Am Chem Soc* 131:4335–4345.
13. Tilset M (2001) The thermodynamics of organometallic systems involving electron transfer paths. *Electron Transfer in Chemistry*, ed Balzani V (Wiley-VCH, Weinheim), Vol. 2, pp. 677–713.
14. Borges dos Santos RM, Martinho Simões JA (1998) Energetics of the O-H bond in phenol and substituted phenols: A critical evaluation of literature data. *J Phys Chem Ref Data* 27:707–739.
15. Mulder P, et al. (2005) Critical re-evaluation of the O-H bond dissociation enthalpy in phenol. *J Phys Chem A* 109:2647–2655.
16. Bernhard K, et al. (2001) Photo- and radiation-chemical formation and electrophilic and electron transfer reactivities of enolether radical cations in aqueous solution. *Chem Eur J* 7:4640–4650.
17. Steenken S, Neta P (1982) One-electron redox potentials of phenols. Hydroxy- and aminophenols and related compounds of biological interest. *J Phys Chem* 86:3661–3667.
18. Snelgrove DW, Jusztyk J, Banks JT, Mulder P, Ingold KU (2001) Kinetic solvents effects on hydrogen-atom abstractions: Reliable, quantitative predictions via a single empirical equation. *J Am Chem Soc* 123:469–477.
19. Borges dos Santos RM, Costa Cabral BJ, Martinho Simões JA (2007) Bond-dissociation enthalpies in the gas phase and in organic solvents: Making ends meet. *Pure Appl Chem* 79:1369–1382.
20. Berthelot M, Besseau F, Laurence C (1998) The hydrogen-bond basicity pK_{HB} scale of peroxides and ethers. *Eur J Org Chem* 1998:925–931.
21. Roduner E (2005) Hydrophobic solvation, quantum nature and diffusion of atomic hydrogen in liquid water. *Rad Phys Chem* 72:201–206.
22. Lind J, Shen X, Eriksen TE, Merényi G (1990) The one-electron reduction potential of 4-substituted phenoxyl radicals in water. *J Am Chem Soc* 112:479–482.
23. Foti M, Ingold KU, Lusztyk J (1994) The surprisingly high reactivity of phenoxyl radicals. *J Am Chem Soc* 116:9440–9447.
24. Das TN, Neta P (1998) Reduction potentials of napthoxyl and pyridoxyl radicals in aqueous solutions. *J Phys Chem A* 102:7081–7085.
25. Lind J, Shen X, Eriksen TE, Merényi G (1989) The one-electron potential of 4-substituted phenoxyl radicals in water. *J Am Chem Soc* 112:479–482.
26. Perrin DD (1965) *Dissociation Constants of Organic Bases in Aqueous Solution* (Butterworth, Washington, DC).
27. Neta P, Grodowski J (2005) Rate constants for reactions of phenoxyl radicals in solution. *J Phys Chem Ref Data* 34:109–199.
28. Roth JP, Yoder JC, Won TJ, Mayer JM (2001) Application of the Marcus cross relation to hydrogen atom transfer reactions. *Science* 294:2524–2526.
29. Heneghan SP, Benson SW (1983) Kinetics and equilibria in the system $Br + t\text{-}BuO_2H \leftrightarrows HBr + t\text{-}BuO_2$. OH bond dissociation energy in $t\text{-}BuO_2\text{-}H$. *Int J Chem Kinet* 15:815–822.
30. Simmie JM, Black G, Curran HJ, Hinde JP (2008) Enthalpies of formation and bond dissociation energies of lower alkyl hydroperoxides and related hydroperoxy and alkoxy radicals. *J Phys Chem A* 112:5010–5016.
31. Chase MW, Jr (1998) NIST-JANAF Thermochemical Tables, Fourth Edition. *J Phys Chem Ref Data*, Monograph 9:1–1951.
32. Khursan SL, Martem'yanov VS (1991) Thermochemistry of the recombination of peroxyl radicals (Translated from Russian). *Russ J Phys Chem* 65:321–325.
33. Blanksby SJ. et al. (2001) Negative-ion photoelectron spectroscopy, gas phase acidity, and thermochemistry of the peroxyl radicals CH_3OO and CH_3CH_2OO. *J Am Chem Soc* 123:9585–9596.
34. Clifford EP, et al. (1998) Photoelectron spectroscopy, pas phase acidity and thermochemistry of *tert*-butyl hydroperoxide: Mechanisms for the rearrangement of peroxyl radicals. *J Chem Phys* 109:10293–10310.
35. Mugnaini V, Lucarini M (2007) Hydrogen bonding affects the persistancy of peroxyl radicals. *Org Lett* 9:2725–2728.
36. Chenier JHB, Howard JA (1975) Kinetic electron spin resonance study of the transfer of a hydrogen atom from α-tetralin hydroperoxide to a tertiary alkylperoxy radical. *Can J Chem* 53:623–627.
37. Ervin KM, DeTuri VF (2002) Anchoring the gas-phase acidity scale. *J Phys Chem A* 106:9947–9956.
38. Griller D, Ingold KU (1974) Abstraction of the hydroxylic hydrogen of alcohols by alkoxy radicals. *J Am Chem Soc* 96:630–632.
39. Warren JJ, Mayer JM (2008) Surprisingly long-lived ascorbyl radicals in acetonitrile: Hydrogen atom transfer reactions and thermochemistry. *J Am Chem Soc* 130:2774–2776.
40. Creutz C (1981) The complexities of ascorbate as a reducing agent. *Inorg Chem* 20:4449–4452.
41. Mader EA, Larsen AS, Mayer JM (2004) Hydrogen atom transfer from iron(II)-Tris[2,2′-bi(tetrahydropyrimidine)] to TEMPO: A negative enthalpy of activation predicted by the Marcus equation. *J Am Chem Soc* 126:8066–8067.
42. Warren JJ, Mayer JM (2008) Surprisingly long-lived ascorbyl radicals in acetonitrile: Hydrogen atom transfer reactions and thermochemistry. *J Am Chem Soc* 130:2774–2776.
43. Ellison GB, Davico GE, Bierbaum VM, DePuy CH (1996) Thermochemistry of the benzyl and allyl radicals and ions.*Int J Mass Spectrom* 156:109–131.
44. Jackson RA, O'Neill DW (1969) The Reaction of benzyl radicals with *m*-deuteriotoluene. *J Chem Soc Chem Commun* 1969:1210–1211.
45. Bordwell FG, Cheng J-P, Ji G-Z, Satish AV, Zhang X (1991) Bond dissociation energies in DMSO related to the gas phase. *J Am Chem Soc* 113:9790–9795.
46. Bryant JR (2002) Mechanistic studies of the oxidations of hydrocarbons by manganese and ruthenium transition metal complexes. PhD thesis (University of Washington, Seattle).
47. See ref. 42 (and its Supporting Information) for a summary of TEMPOH and ${}^t\mathrm{Bu_3PhOH}$ thermochemistry.
48. Burton GW, et al. (1985) Autoxidation of biological molecules. 4. Maximizing the antioxidant activity of phenols. *J Am Chem Soc* 107:7053–7065.
49. Wantanbe A, et al. (2000) Stability and reactivity of aryloxyl radicals derived from a novel antioxidant BO-653 and related compounds. Effects of substituent and side chain in solution membranes. *J Am Chem Soc* 122:5438–5442.
50. Mahoney LR, DaRooge MA (1970) The equilibrium reaction of 2,4,6-Tri-*t*butylphenol and organic peroxy radicals. *J Am Chem Soc* 92:4063–4067.
51. Howard JA, Furimsky E (1973) Arrhenius parameters for reaction of *tert*-butylperoxy radicals with some hindered phenols and aromatic amines. *Can J Chem* 51:3738–3745.
52. Chenier JHB, Furimsky E, Howard JA (1974) Arrhenius parameters for reaction of the *tert*-butylperoxy and 2-ethyl-2-propylperoxy radicals with some nonhindered phenols and aromatic amines. *Can J Chem* 52:3682–3688.
53. Fischer H, ed (1997) *Radical Reaction Rates in Liquids*, Landolt-Börnstein New Series Vol. 18, Subvol. D2 (Springer, New York).
54. Arends IWCE, Mulder P, Clark KB, Wayner DDM (1995) Rate constants for termination and TEMPO trapping of some resonance stabilized hydroaromatic radicals in the liquid phase. *J Phys Chem* 99:8182–8189.
55. Davies MJ, Forni LG, Willson RL (1988) Vitamin E analogue Trolox C ESR and pulse-radiolysis studies of free-radical reactions. *Biochem J* 255:513–522.
56. Mahoney LR, DaRooge MA (1975) The kinetic behavior and thermochemical properties of phenoxy radicals. *J Am Chem Soc* 97:4722–4731.
57. Bisby RH, Parker AW (1995) The reaction of ascorbate with the α-tocopheroxyl radical in micellar and bilayer membrane systems. *Arch Biochem Biophys* 317:170–178.
58. Hunter EPL, Desrosiers MF, Simic MG (1989) The effect of oxygen, antioxidants and superoxide radical on tyrosine phenoxyl radical dimerization. *Free Radical Bio Med* 6:581–585.

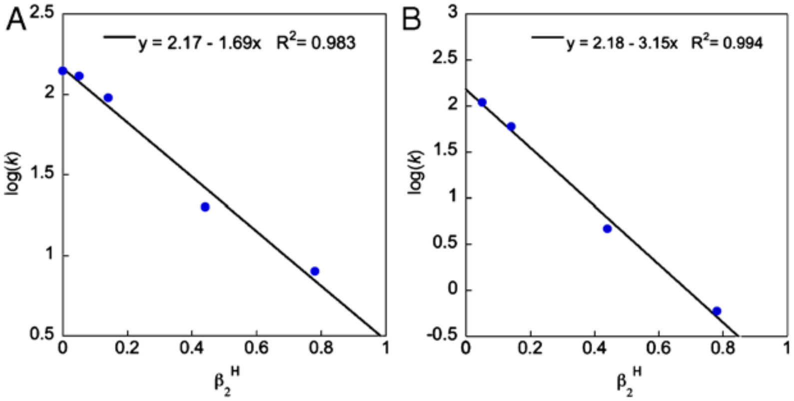

Fig. S1. Plots of $\log(k_{XH/X^\bullet})$ versus $\beta_2{}^H$ for (*a*) ^{t}Bu$_3$PhO($^\bullet$/H) and (*b*) TEMPO($^\bullet$/H). Agreement with the KSE model requires the slopes to be $-8.3\alpha_2{}^H$(XH). For ^{t}Bu$_3$PhOH, for which $\alpha_2{}^H = 0.22 \pm 0.04$ (1), the predicted slope is -1.83 ± 0.33—within error of the observed slope of -1.69 ± 0.26. For TEMPOH [$\alpha_2{}^H = 0.39 \pm 0.05$ (1)], the predicted slope is -3.24 ± 0.41, again within error of the observed slope, -3.15 ± 0.34. Thus this dataset agrees very well with the predictions of the KSE model. (All errors are reported to 2σ.)

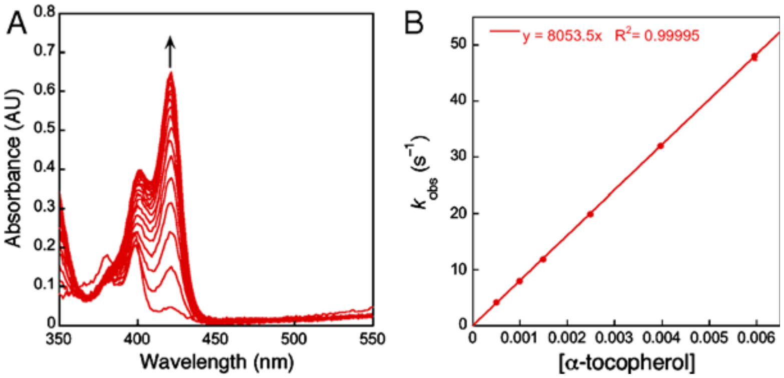

Fig. S2. (*a*) Selected stopped-flow UV-vis spectra for reaction of TocOH (2.5 mM) with ^{t}Bu$_3$PhO$^\bullet$ (0.1 mM) over the course of 0.3 s. (*b*) Plot of pseudo-first-order k_{obs} as a function of [TocOH]. The slope of the line is the second-order rate constant for reaction S3.

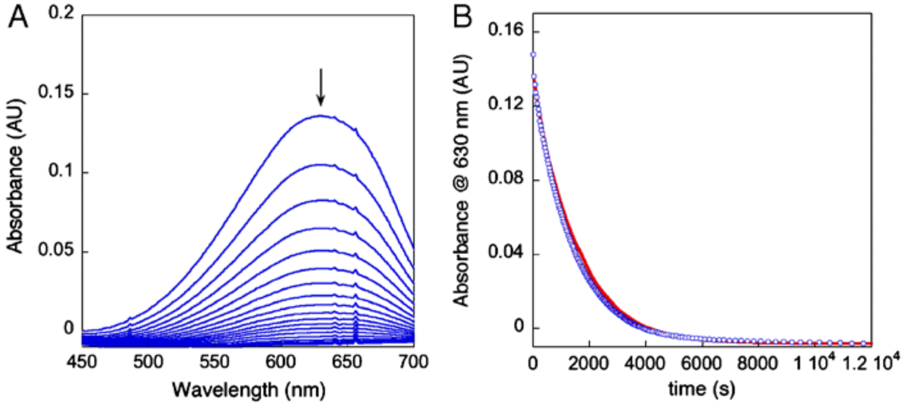

Fig. S3. (*a*) Selected stopped-flow UV-vis spectra for reaction of ^{t}Bu$_3$PhO$^\bullet$ (0.6 mM) with 85.4 mM DHA over 10,500 s. (*b*) Kinetic trace at 632 nm (*Blue Circles*) and resulting fit from an AB kinetic model (*Solid Red Line*).

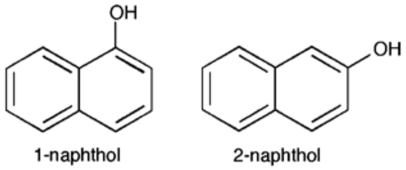

Fig. S4. Chemical structures of 1-naphthol and 2-naphthol.

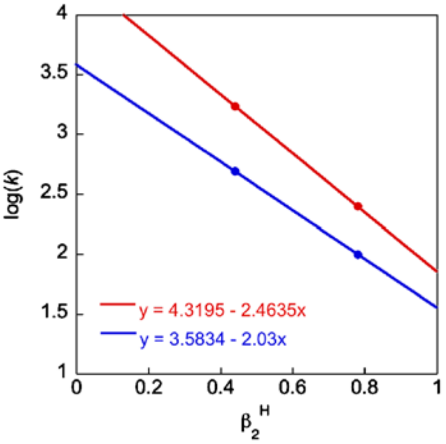

Fig. S5. Plots of $\log(k)$ versus $\beta_2{}^{\mathrm{H}}$ for *i*AscH⁻ + TEMPO (*Red, Top Line*) and AscH⁻ (*Blue, Bottom Line*). Agreement with the KSE model requires the slopes to be to $-8.3\alpha_2{}^{\mathrm{H}}(\mathrm{XH})$.

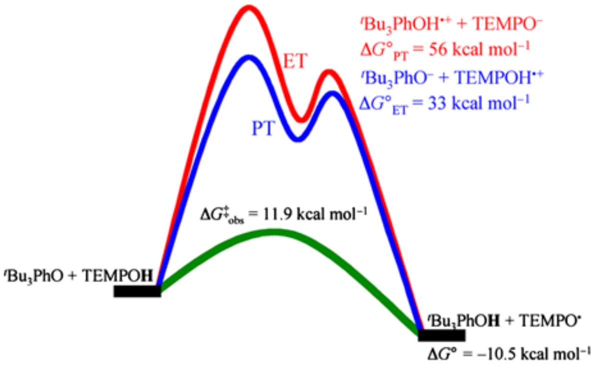

Fig. S6. Thermochemical landscape for stepwise ET-PT, PT-ET, and concerted $H^{\bullet}$ transfer reactions. The free energies of the stepwise PT-first or ET-first intermediates ($\Delta G°_{PT}$ and $\Delta G°_{ET}$, respectively) are calculated from the differences in pK_as or $E_{1/2}$s of ^{t}Bu$_3$PhO$^{\bullet}$ and TEMPOH in MeCN solvent, respectively. The barrier ($\Delta G^{\ddagger}_{obs}$) is calculated from the experimentally measured forward rate constant by using the Eyring equation. Because the free energy to reach the intermediates is much higher than the observed barrier, these reactions proceed via the concerted transfer of $H^{\bullet}$. This same type of scheme can be applied to the degenerate self-exchange reactions as well, showing that they also must proceed by a concerted mechanism.

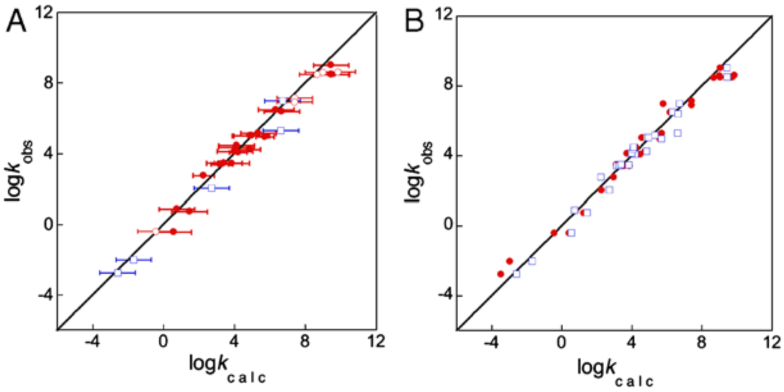

Fig. S7. (*a*) Comparison between experimentally determined HAT rate constants and those determined by using the CR/KSE model with the addition of the solvent correction (C_S) term. All reactions from Table 4 are included: • = RO$^{\bullet}$ + R′O-H cross reactions in aprotic solvents, □ = RO$^{\bullet}$ + R′C-H cross reactions in aprotic solvents, and ◦= RO$^{\bullet}$ + R′O-H cross reactions in protic solvents, *uncorrected* for C_S. The black line indicates perfect agreement. The correlation coefficient (R^2) for all data is 0.97. (*b*) Comparison between CR/KSE calculated self-exchange rate constants corrected for C_S (□) and uncorrected for C_S (•). The black line indicates perfect agreement. For clarity, the error bars are not shown.

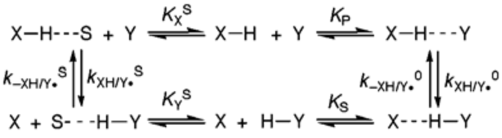

Scheme S1. Equilibria involved in HAT reactions in H-bond accepting solvent *S*.

Table S1. Summary of BDFE and self-exchange rate constants as a function of solvent

Compound	Solvent	BDFE[*]	$k_{\mathrm{XH/X\bullet}}$[*]
${}^{t}Bu_3PhOH$	Alkane	76.0	140[†,‡]
${}^{t}Bu_3PhOH$	CCl_4	76.7	130[‡,§]
${}^{t}Bu_3PhOH$	PhCl	76.7	93[‡]
${}^{t}Bu_3PhOH$	C_6H_6	76.9	95[‡,§]
${}^{t}Bu_3PhOH$	MeCN	77.8	20[‡,§]
${}^{t}Bu_3PhOH$	DMSO	79.2	8[‡,§]
BHT	Alkane	75.8	140[†,‡]
BHT	Styrene	76.7	60[‡]
2, 6-${}^{t}Bu_2PhOH$	Styrene	78.5	60[‡]
2, 6-${}^{t}Bu_2$-4-OMePhOH	C_6H_6	73.9	95[‡,§]
2, 6-${}^{t}Bu_2$-4-OMePhOH	MeCN	74.9	20[‡,§]
2, 6-${}^{t}Bu_2$-4-OMePhOH	DMSO	76.3	8[‡,§]
TEMPOH	CCl_4	65.1	110[†]
TEMPOH	C_6H_6	65.4	60[§]
TEMPOH	MeCN	66.5	4.7[†]
TEMPOH	DMSO	68.8	0.6[§]
*i*AscH$^-$	MeCN	67.6	5.4×10^{5}[†]
AscH$^-$	Water	73.6	3×10^{5}
Trolox C	Water	78.5	3.4×10^{4}
Tyrosine	Water	87.8	6.4×10^{4}
${}^{t}BuOOH$	Alkane	80.4	500[†]
${}^{t}BuOOH$	Styrene	81.7	110
${}^{t}BuOOH$	Toluene	81.5	150
${}^{t}BuOOH$	PhCl	81.3	230
${}^{t}BuOOH$	Ethanol	82.6	12
PhOH	Alkane	84.9	5×10^{7}
PhOH	PhCl	85.9	1.7×10^{7}
PhOH	DTBP	87.8	9.0×10^{5}
PhOH	Water	90.1	6.4×10^{5}
TocOH	Styrene	74.0	1.5×10^{5}
TocOH	Ethanol	74.1	2.2×10^{4}
TocOH	DTBP	75.0	4.2×10^{4}
${}^{t}BuOH$	DTBP	104.4	3×10^{4}[†]
9,10-dihydroanthracene	PhCl	74.6	5×10^{-11}
9,10-dihydroanthracene	MeCN	75.0	5×10^{-11}
9,10-dihydroanthracene	DTBP	75.0	5×10^{-11}
Toluene	Toluene	86.4	8×10^{-5}[†]
Toluene	DTBP	86.8	8×10^{-5}

[*] $k_{\mathrm{XH/X\bullet}}$ in $M^{-1}\,s^{-1}$ at 298 K and BDFE in kcal mol^{-1}. BDFEs are from solution $E_{1/2}$ and pK_a data or have been corrected by using the Abraham model as outlined for each compound as described above.

[†] Directly measured [see above for references].

[‡] Self-exchange rate constants for 2,6-*tert*-butyl substituted phenols are not expected to change drastically with the 4-substituent.

[§] Directly measured (this work).

Table S2. Summary of observed and calculated (Eq. 2) hydrogen transfer rate constants

Entry	Reaction ($XH + Y^{\bullet}$)	Solvent (β_2^{H})[*]	$K_{XH/Y^{\bullet}}$[†]	k_{obs}[‡]	k_{calc}[‡]	Ref.
1[§]	TEMPOH + ${}^{t}\mathrm{Bu_3PhO}^{\bullet}$	MeCN (0.44)	5.0×10^{7}	1.25×10^{4}	2.9×10^{4}	¶
2[§]	TEMPOH + ${}^{t}\mathrm{Bu_3PhO}^{\bullet}$	DMSO (0.78)	4.7×10^{7}	2.7×10^{3}	7.2×10^{3}	¶
3[§]	TEMPOH + ${}^{t}\mathrm{Bu_3PhO}^{\bullet}$	C_6H_6 (0.14)	2.4×10^{8}	9.5×10^{4}	2.2×10^{5}	¶
4[§]	TEMPOH + ${}^{t}\mathrm{Bu_3PhO}^{\bullet}$	CCl_4 (0.05)	2.7×10^{8}	9.5×10^{4}	2.2×10^{5}	¶
5[§]	TEMPOH + ${}^{t}\mathrm{Bu_2MeOPhO}^{\bullet}$	MeCN (0.44)	3.2×10^{5}	2.67×10^{3}	3.5×10^{3}	¶
6[§]	TEMPOH + ${}^{t}\mathrm{Bu_2MeOPhO}^{\bullet}$	DMSO (0.78)	3.4×10^{4}	6.2×10^{2}	8.3×10^{2}	¶
7[§]	TEMPOH + ${}^{t}\mathrm{Bu_2MeOPhO}^{\bullet}$	C_6H_6 (0.14)	1.8×10^{6}	1.85×10^{4}	2.7×10^{4}	¶
8[§]	$i\mathrm{AscH}^{-}$ + ${}^{t}\mathrm{Bu_3PhO}^{\bullet}$	MeCN (0.44)	2.3×10^{8}	3.4×10^{6}	1.3×10^{7}	42
9[§]	$i\mathrm{AscH}^{-}$ + ${}^{t}\mathrm{Bu_2MeOPhO}^{\bullet}$	MeCN (0.44)	1.5×10^{6}	5.3×10^{5}	1.9×10^{6}	42
10	${}^{t}\mathrm{Bu_2MeOPhOH}$ + $\mathrm{ROO}^{\bullet}$[‖]	Styrene (0.18)	4.5×10^{5}	1.1×10^{5}	4.1×10^{4}	48
11	BHT + $\mathrm{ROO}^{\bullet}$[‖]	Styrene (0.18)	4.7×10^{3}	1.4×10^{4}	5.6×10^{3}	48
12	2, 6-${}^{t}\mathrm{Bu_2PhOH}$ + $\mathrm{ROO}^{\bullet}$[‖]	Styrene (0.18)	2.3×10^{2}	3.1×10^{3}	1.4×10^{3}	48
13	TocOH + $\mathrm{ROO}^{\bullet}$[‖]	Styrene (0.18)	4.8×10^{5}	3.2×10^{6}	1.8×10^{6}	48
14[§]	${}^{t}\mathrm{Bu_2MeOPhOH}$ + $\mathrm{ROO}^{\bullet}$	Alkane[**] (0)	2.4×10^{5}	1.1×10^{5}	8.8×10^{4}	48
15[§]	BHT + ${}^{t}\mathrm{BuOO}^{\bullet}$	Alkane[**] (0)	2.5×10^{3}	2.4×10^{4}	1.2×10^{4}	48
16	TocOH + ${}^{t}\mathrm{BuOO}^{\bullet}$	Alkane[**] (0)	4.0×10^{5}	2.6×10^{6}	3.8×10^{6}	48
17	${}^{t}\mathrm{BuOOH}$ + $\mathrm{TocO}^{\bullet}$	Ethanol (0.44)	1.5×10^{-6}	4.1×10^{-1}	3.8×10^{-1}	49
18	Tetralin hydroperoxide + ${}^{t}\mathrm{Bu_3PhO}^{\bullet}$	PhCl (0.11)	4.2×10^{-4}	3.4×10^{-1}	2	50
19	PhOH + ${}^{t}\mathrm{Bu_3PhO}^{\bullet}$	Hexane (0)	3.1×10^{-7}	5.7	19	4
20	1-NapOH + ${}^{t}\mathrm{BuOO}^{\bullet}$	Isopentane (0)	3.5×10^{0}	1.5×10^{5}	5.3×10^{5}	51
21	2-NapOH + ${}^{t}\mathrm{BuOO}^{\bullet}$	Isopentane (0)	1.4×10^{-2}	3.1×10^{4}	1.7×10^{4}	52
22	PhOH + ${}^{t}\mathrm{BuOO}^{\bullet}$	Heptane (0)	5.5×10^{-4}	3×10^{3}	2.8×10^{3}	53
23[§]	PhOH + ${}^{t}\mathrm{BuO}^{\bullet}$	DTBP:C_6H_6	1.6×10^{12}	3.3×10^{8}	5.9×10^{9}	54
24[§]	TocOH + $\mathrm{PhO}^{\bullet}$	2:1 DTBP:MeCN	2.6×10^{9}	3.2×10^{8}	1.2×10^{9}	23
25[§]	TocOH + $\mathrm{PhO}^{\bullet}$	3:1 DTBP:C_6H_6	2.6×10^{9}	1.1×10^{9}	1.2×10^{9}	23
26	Trolox C + $\mathrm{PhO}^{\bullet}$	Water (0.38)	1.0×10^{8}	4.1×10^{8}	9.7×10^{8}	55
27	PhOH + ${}^{t}\mathrm{Bu_3PhO}^{\bullet}$	PhCl (0.09)	1.8×10^{-7}	<8[††]	6.6	56
28	AscH^{-} + Trolox C radical	Water (0.38)	4.7×10^{3}	1.4×10^{7}	2.5×10^{7}	57
29	AscH^{-} + Trolox C radical	Water (0.38)	4.7×10^{3}	8.3×10^{6}	2.5×10^{7}	55
30	AscH^{-} + tyrosyl radical	Water (0.38)	4.0×10^{10}	4.4×10^{8}	7.0×10^{9}	58
31	Trolox C + tyrosyl radical	Water (0.38)	9.3×10^{6}	3.1×10^{8}	4.5×10^{8}	58
32	DHA + $\mathrm{PhO}^{\bullet}$	PhCl (0.09)	1.9×10^{8}	$<1.1 \times 10^{2}$[††]	2.1×10^{2}	56
33[§]	DHA + ${}^{t}\mathrm{Bu_3PhO}^{\bullet}$	MeCN (0.44)	1.2×10^{2}	1.8×10^{-3}	3.3×10^{-4}	¶
34[§]	DHA + ${}^{t}\mathrm{BuO}^{\bullet}$	DTBP:C_6H_6	9×10^{21}	9.5×10^{6}	7.9×10^{5}	54
35[§]	Toluene + ${}^{t}\mathrm{BuO}^{\bullet}$	DTBP:C_6H_6	8.9×10^{12}	2.3×10^{5}	3.4×10^{5}	54
36	Toluene + ${}^{t}\mathrm{BuOO}^{\bullet}$	Toluene (0.14)	2.6×10^{-4}	1×10^{-2}	1.5×10^{-3}	53

[*] β_2^{H} values from ref. 9 (above).

[†] $K_{XH/Y^{\bullet}}$ in organic solvents corrected by using the Abraham model. $K_{XH/Y^{\bullet}}$ in water from thermochemical cycles.

[‡] This table corresponds to Table 4 in the main text. k in $M^{-1}\,s^{-1}$ at 298 K unless otherwise noted.

[§] Indicates both $k_{XH/X^{\bullet}}$ and $k_{YH/Y^{\bullet}}$ are known in the given solvent.

[¶] This work.

[‖] $\mathrm{ROO}^{\bullet}$ = polyperoxystyryl.

[**] Alkane = decane or cyclohexane.

[††] Rate constant measured at 333 K.

Table S3. Summary of C_S values and C_S-corrected rate constants

Entry	Reaction ($XH + Y^{\bullet}$)	Solvent (β_2^{H})	$\log(C_S)$	k_{obs}[*]	$k_{calc,corrected}$[*]
1[†]	TEMPOH + $^{t}Bu_3PhO^{\bullet}$	MeCN (0.44)	−0.29	1.25×10^{4}	1.5×10^{4}
2[†]	TEMPOH + $^{t}Bu_3PhO^{\bullet}$	DMSO (0.78)	−0.71	2.7×10^{3}	1.4×10^{3}
3[†]	TEMPOH + $^{t}Bu_3PhO^{\bullet}$	C_6H_6 (0.14)	8.8×10^{-2}	9.5×10^{4}	4.9×10^{5}
4[†]	TEMPOH + $^{t}Bu_3PhO^{\bullet}$	CCl_4 (0.05)	0.20	9.8×10^{4}	9.9×10^{5}
5[†]	TEMPOH + $^{t}Bu_2MeOPhO^{\bullet}$	MeCN (0.44)	−0.29	2.67×10^{3}	1.8×10^{3}
6[†]	TEMPOH + $^{t}Bu_2MeOPhO^{\bullet}$	DMSO (0.78)	−0.71	6.2×10^{2}	1.7×10^{2}
7[†]	TEMPOH + $^{t}Bu_2MeOPhO^{\bullet}$	C_6H_6 (0.14)	8.8×10^{-2}	1.85×10^{4}	6.9×10^{4}
8[†]	*i*AscH^{-} + $^{t}Bu_3PhO^{\bullet}$	MeCN (0.44)	-[‡]	3.4×10^{6}	-[‡]
9[†]	*i*AscH^{-} + $^{t}Bu_2MeOPhO^{\bullet}$	MeCN (0.44)	-[‡]	5.3×10^{5}	-[‡]
10	$^{t}Bu_2MeOPhOH$ + $ROO^{\bullet}$	Styrene (0.18)	0.29	1.1×10^{5}	7.2×10^{4}
11	BHT + $ROO^{\bullet}$	Styrene (0.18)	0.29	1.4×10^{4}	9.8×10^{3}
12	2, 6-$^{t}Bu_2PhOH$ + $ROO^{\bullet}$	Styrene (0.18)	0.29	3.1×10^{3}	2.5×10^{3}
13	TocOH + $ROO^{\bullet}$	Styrene (0.18)	0.15	3.2×10^{6}	2.1×10^{6}
14[†]	$^{t}Bu_2MeOPhOH$ + $ROO^{\bullet}$	Alkane (0)	-5.9×10^{-3}	1.1×10^{5}	8.7×10^{4}
15[†]	BHT + $^{t}BuOO^{\bullet}$	Alkane (0)	-5.9×10^{-3}	2.4×10^{4}	1.2×10^{4}
16	TocOH + $^{t}BuOO^{\bullet}$	Alkane (0)	5.8×10^{-2}	2.6×10^{6}	4.4×10^{6}
17	$^{t}BuOOH$ + $TocO^{\bullet}$	Ethanol (0.44)	-[‡]	4.1×10^{-1}	-[‡]
18	Tetralin hydroperoxide + $^{t}Bu_3PhO^{\bullet}$	PhCl (0.11)	0.14	3.4×10^{-1}	3.5
19	PhOH + $^{t}Bu_3PhO^{\bullet}$	Hexane (0)	0.20	5.7	27
20	1-NapOH + $^{t}BuOO^{\bullet}$	Isopentane (0)	−0.14	1.5×10^{5}	2.1×10^{5}
21	2-NapOH + $^{t}BuOO^{\bullet}$	Isopentane (0)	−0.14	3.1×10^{4}	1.2×10^{4}
22	PhOH + $^{t}BuOO^{\bullet}$	Heptane (0)	0.36	3×10^{3}	6.5×10^{3}
23[†]	PhOH + $^{t}BuO^{\bullet}$	DTBP:C_6H_6	−0.24	3.3×10^{8}	3.0×10^{9}
24[†]	TocOH + $PhO^{\bullet}$	2:1 DTBP:MeCN	0.39	3.2×10^{8}	2.6×10^{9}
25[†]	TocOH + $PhO^{\bullet}$	3:1 DTBP:C_6H_6	0.39	1.1×10^{9}	2.6×10^{9}
26	Trolox C + $PhO^{\bullet}$	Water (0.38)	-[‡]	4.1×10^{8}	-[‡]
27	PhOH + $^{t}Bu_3PhO^{\bullet}$	PhCl (0.09)	-6.1×10^{-2}	<8	5.3
28	AscH^{-} + Trolox C radical	Water (0.38)	-[‡]	1.4×10^{7}	-[‡]
29	AscH^{-} + Trolox C radical	Water (0.38)	-[‡]	8.3×10^{6}	-[‡]
30	AscH^{-} + tyrosyl radical	Water (0.38)	-[‡]	4.4×10^{8}	-[‡]
31	Trolox C + tyrosyl radical	Water (0.38)	-[‡]	3.1×10^{8}	-[‡]
32	DHA + $PhO^{\bullet}$	PhCl (0.09)	0.45	$<1.1 \times 10^{2}$	5.1×10^{2}
33[†]	DHA + $^{t}Bu_3PhO^{\bullet}$	MeCN (0.44)	0.88	1.0×10^{-3}	2.5×10^{-3}
34[†]	DHA + $^{t}BuO^{\bullet}$	DTBP:C_6H_6	0.93	9.5×10^{6}	5.3×10^{6}
35[†]	Toluene + $^{t}BuO^{\bullet}$	DTBP:C_6H_6	0.93	2×10^{5}	4.2×10^{6}
36	Toluene + $^{t}BuOO^{\bullet}$	Toluene (0.14)	1.3	1×10^{-2}	2.0×10^{-2}

[*] This table corresponds to Table 4 (main text) and Table S2 (above). C_S values were calculated as described above. Rate constants are in $M^{-1}\,s^{-1}$. Data in protic solvents are not included.

[†] Indicates both $k_{XH/X^{\bullet}}$ and $k_{YH/Y^{\bullet}}$ are known in the given solvent.

[‡] Not calculated. $\beta_2^{H}(RO^{\bullet})$ is unknown and cannot be estimated by analogy to other compounds.